OXFORD

Human Molecular Genetics, 2023, Vol. 32, 7, 1114–1126
https://doi.org/10.1093/hmg/ddac273
Advance access publication date 2 November 2022
Original Article

Transcription factor FoxM1 promotes cyst growth in PKD1 mutant ADPKD

Wenyan Yu[1,2,3,†], Guojuan Wang[1,2,4,†], Linda Xiaoyan Li[1,2], Hongbing Zhang[1,2,6], Xuehong Gui[1,2], Julie Xia Zhou[1,2], James P. Calvet[3] and Xiaogang Li[1,2,*]

[1]Department of Internal Medicine, Mayo Clinic, Rochester, MN 55905, USA
[2]Department of Biochemistry and Molecular Biology, Mayo Clinic, Rochester, MN 55905, USA
[3]Research Center for Differentiation and Development of TCM Basic Theory, Jiangxi Province Key Laboratory of TCM Etiopathogenesis, Jiangxi University of Chinese Medicine, Nanchang, Jiangxi 330004, China
[4]Department of Oncology, The Affiliated Hospital of University of Jiangxi of Traditional Chinese Medicine, Nanchang 330006, China
[5]Department of Biochemistry and Molecular Biology, University of Kansas Medical Center, Kansas City, KS 66160, USA
[6]Eye Institute of Shaanxi Province; Xi'an First Hospital, Xi'an 710002, Shaanxi Province, China
*To whom correspondence should be addressed at: Department of Medicine, Biochemistry and Molecular Biology, Mayo Clinic, 200 1st Street, SW, Rochester, MN 55905, USA. Tel: +1 507-266-0110; Email: li.xiaogang@mayo.edu
†These authors contributed equally to this study.

Abstract

Autosomal dominant polycystic kidney disease (ADPKD) is driven by mutations in the *PKD1* and *PKD2* genes, and it is characterized by renal cyst formation, inflammation and fibrosis. Forkhead box protein M1 (FoxM1), a transcription factor of the Forkhead box (Fox) protein super family, has been reported to promote tumor formation, inflammation and fibrosis in many organs. However, the role and mechanism of FoxM1 in regulation of ADPKD progression is still poorly understood. Here, we show that FoxM1 is an important regulator of cyst growth in ADPKD. FoxM1 is upregulated in cyst-lining epithelial cells in *Pkd1* mutant mouse kidneys and human ADPKD kidneys. FoxM1 promotes cystic renal epithelial cell proliferation by increasing the expression of Akt and Stat3 and the activation of ERK and Rb. FoxM1 also regulates cystic renal epithelial cell apoptosis through NF-κB signaling pathways. In addition, FoxM1 regulates the recruitment and retention of macrophages in *Pkd1* mutant mouse kidneys, a process that is associated with FoxM1-mediated upregulation of monocyte chemotactic protein 1. Targeting FoxM1 with its specific inhibitor, FDI-6, delays cyst growth in rapidly progressing and slowly progressing *Pkd1* mutant mouse kidneys. This study suggests that FoxM1 is a central and upstream regulator of ADPKD pathogenesis and provides a rationale for targeting FoxM1 as a therapeutic strategy for ADPKD treatment.

Introduction

Autosomal dominant polycystic kidney disease (ADPKD) is an inherited genetic disease caused by mutations in one of two genes, *PKD1* or *PKD2*, which encode the proteins polycystin-1 (PC1) and polycystin-2 (PC2), respectively (1). With an inherited autosomal dominant trait in families, an individual can inherit the PKD gene mutation, or defect, from only one parent (2). ADPKD can also occur in an individual without a family history of ADPKD, resulting from a new genetic mutation in one of the ADPKD genes (3). ADPKD is a progressive disease and symptoms vary in age of onset and severity, and tend to get worse over time. The most common symptoms of ADPKD are kidney cysts, pain in the back and sides and headaches. Other symptoms include high blood pressure (hypertension), blood in the urine (hematuria), recurrent urinary tract infections, kidney stones, heart valve abnormalities and brain aneurysms. About half of people with ADPKD will develop kidney failure in adulthood, requiring kidney dialysis and/or kidney transplantation (4). The diagnosis of ADPKD is based on the symptoms, clinical examination, family history and imaging studies of the kidneys. Genetic testing can also be used to help confirm the diagnosis. Treatment for ADPKD involves managing the symptoms (both kidney and non-kidney symptoms) and slowing disease progression. To slow disease progression will require a comprehensive understanding of the molecular mechanisms of ADPKD. Diverse PKD-associated signaling pathways have been identified in the regulation of cystic renal epithelial cell proliferation and apoptosis and ferroptosis as well as renal inflammation and fibrosis (5,6). However, the roles and mechanisms of one of the key transcriptional factors, forkhead box protein M1 (FOXM1), in ADPKD remain elusive.

FOXM1 is a critical proliferation-associated transcription factor of the forkhead box (Fox) protein superfamily with a central role in a wide range of biological processes, including embryonic and fetal development as well as adult tissue homeostasis and repair (7,8). The FOXM1 protein contains a conserved forkhead DNA-binding domain (DBD), an N-terminal repressor domain (NRD) and a C-terminal acidic transactivation domain (TAD). The transactivation activity of TAD can be suppressed by direct interaction with the NRD (9). Murine FoxM1 displays the same DNA-binding specificity as human FOXM1, which can bind to DNA-binding sites with the consensus sequence 5′-A-C/T-AAA-C/T-AA-3′ (10), suggesting that FOXM1 of the two species may share target genes. This would suggest that the study of murine FOXM1 may apply to human FOXM1, and that the mouse is a suitable experimental model for the mechanistic investigation of FOXM1 in disease and the development of novel FOXM1 inhibitors.

Received: August 28, 2022. **Revised:** October 27, 2022. **Accepted:** October 28, 2022

During the cell cycle, FOXM1 promotes the entry of S-phase and M-phase by regulating the expression of genes, whose products control the G1/S-transition, S-phase progression, G2/M-transition and M-phase progression. Additionally, FOXM1 regulates a network of proliferation-associated genes critical to mitotic spindle assembly and chromosome segregation, and depletion of FoxM1 results in cell cycle arrest (9). FOXM1 also targets genes involved in differentiation, senescence, stem cell renewal, DNA damage response, attenuation of oxidative stress, epithelial–mesenchymal transition (EMT), angiogenesis, metastasis and pre-metastatic niche formation (11,12). Aberrant up-regulation of FOXM1 has been shown to be a key driver of cancer progression and has been proposed as an initiating factor of oncogenesis (13). It is apparent that the inhibition of FOXM1 expression (at the levels of transcription, translation or post-translationally) and/or its interactions with target sites (by blocking the DBD, nuclear localization or other protein–protein interactions) may be effective ways to inhibit FOXM1-mediated biological effects. The pharmacological inhibition of FOXM1 in cancer has been successful (9).

In this study, we have shown that the expression of FoxM1 is elevated in *Pkd1* mutant renal epithelial cells and tissues. The upregulation of FoxM1 was shown to promote cystic epithelial cell proliferation, inhibit cystic epithelial cell apoptosis and increase the recruitment and retention of macrophages through several mechanisms in *Pkd1* mutant mouse kidneys. Targeting FoxM1 with its specific inhibitor, FDI-6, delayed cyst growth, suggesting that FOXM1 inhibition may be a novel therapeutic approach for the treatment of ADPKD with the potential for translation into the clinic.

Results

The expression of FoxM1 is upregulated in *Pkd1* mutant renal epithelial cells and ADPKD tissues

To understand the role of FoxM1 in ADPKD, we first examined expression levels. FoxM1 expression was found to be upregulated in *Pkd1* null mouse embryonic kidney (MEK) collecting duct cells and postnatal *Pkd1* homozygous mutant proximal tubule PN24 cells compared to *Pkd1* wild-type (WT) MEK cells and postnatal *Pkd1* heterozygous PH2 cells as examined by Western blot (Fig. 1A) and quantitative real-time PCR (qRT-PCR) analysis (Fig. 1B). The expression of FoxM1 protein was also increased over time in day 7, day 14 and day 21 kidneys from $Pkd1^{fl/fl}$:*Pkhd1-Cre* mice (Fig. 1C–F), a *Pkd1* conditional knockout mouse model in which cyst growth is initiated around postnatal day 8 and passes the critical time point at postnatal day 14, following by a rapid cyst progression period (14). The upregulation of FoxM1 was detected in collecting ducts (marked by DBA) and proximal tubules (marked by LTL) in kidneys of $Pkd1^{fl/fl}$:*Pkhd1-Cre* and tamoxifen induced $Pkd1^{fl/fl}$:*Tam-Cre* mice compared to control mice as examined by immunofluorescence (IF) staining (Fig. 1G and H). The expression of FoxM1 was also increased in the cyst-lining epithelial cells of *Pkd1* mutant mouse kidneys and human ADPKD patient kidneys compared to that in normal kidneys as examined with immunohistochemistry (IHC) staining (Fig. 1I and J).

Treatment with a specific FoxM1 inhibitor, FDI-6, delays cyst growth in *Pkd1* mutant kidneys

Given that FoxM1 was upregulated in cystic renal epithelial cells and tissues, we investigated whether targeting FoxM1 with its specific inhibitor, FDI-6, would delay cyst growth *in vivo*. We first treated $Pkd1^{nl/nl}$ mice, a hypomorphic *Pkd1* mouse model with cyst development at early stage, with FDI-6 (5 mg/kg) ($n=6$) or vehicle ($n=6$) by daily intraperitoneal (IP) injection from post-natal day 7 (PN7) to PN21 and sacrificed the mice at PN22. The dosage, route and time frames of FDI-6 administration in *Pkd1* mutant mice were based on previous publications (15). We found that treatment with FDI-6 ($n=6$) decreased cystic index (Fig. 2A–C), kidney weight/body weight (KW/BW) ratios (Fig. 2D) and blood urea nitrogen (BUN) levels (Fig. 2E) in the $Pkd1^{nl/nl}$ mice compared to vehicle treated control animals. Furthermore, we found that treatment with FDI-6 decreased cyst-lining epithelial cell proliferation as analyzed by Ki67 staining (Fig. 2F), and increased cyst-lining epithelial cell apoptosis as analyzed by the terminal-deoxynucleotidyl transferase dUTP nick end labeling (TUNEL) assay (Fig. 2G) in kidneys from $Pkd1^{nl/nl}$ mice.

To extend the translational significance of the *in vivo* findings in the younger $Pkd1^{nl/nl}$ mice, we also tested the effects of FDI-6 on renal cyst growth in $Pkd1^{fl/fl}$:*Tam-Cre* mice, in which the Cre is driven by the $Esr1^{+}$ promoter at a later stage (16). We induced *Pkd1* deletion with tamoxifen, and then administered FDI-6 (10 mg/kg) ($n=6$) to these mice through intraperitoneal injection up to 6 months (Fig. 3A) (see Materials and Methods) (16). We found that treatment with FDI-6 delayed cyst growth as seen by decreased of cyst index, KW/BW ratios, BUN levels, cyst-lining epithelial cell proliferation and increased cyst-lining epithelial cell apoptosis (Fig. 3B–I). These results suggest that targeting FoxM1 with pharmacological inhibition might delay cyst growth in ADPKD patients.

FoxM1 regulates renal epithelial cell proliferation through the activation of PKD associated signaling pathways in *Pkd1* mutant renal epithelial cells and kidneys

FoxM1 can directly or indirectly activate the expression of target genes at the transcriptional level to regulate cell proliferation (13). We found that knockdown of FoxM1 with siRNA and inhibition of FoxM1 with its inhibitor FDI-6 decreased the expression and/or the phosphorylation of Akt, ERK, Rb and Stat3 as well as the expression of CDK6 and Plk1 but increased the expression of p21 in PN24 cells (Fig. 4A and B). We also found that treatment with FDI-6 decreased the expression and/or the phosphorylation of Akt, ERK, Rb and Stat3 as well as the expression of CDK6 and Plk1, but increased the expression of p21 in $Pkd1^{fl/fl}$:*Tam-Cre* kidneys (Fig. 4C). In addition, treatment with FDI-6 decreased the expression of FoxM1 in *Pkd1* mutant renal epithelial cells and kidneys of $Pkd1^{fl/fl}$:*Tam-Cre* mice (Fig. 4B and C). These results suggest that FoxM1 is able to regulate multiple PKD associated signaling pathways to promote cystic epithelial cell proliferation and cyst growth.

Inhibition of FoxM1 induces *Pkd1* mutant renal epithelial cell apoptosis via NF-κB signaling

Treatment with FDI-6 was also found to induce cyst-lining epithelial cell death in *Pkd1* knockout kidneys (Figs 2G and 3I). Inhibition of FoxM1 with FDI-6 also induced *Pkd1* homozygous PN24 cell apoptosis as analyzed by TUNEL assay (Fig. 5A) and characterized by the increase of active caspase 3 in FDI-6 treated PN24 cells (Fig. 5B). The activation of caspase-3 was further confirmed by the appearance of cleaved poly (ADP-ribose) polymerase (PARP), a substrate of caspase-3 (Fig. 5B) (17). These results suggest a beneficial role of FDI-6 in induction of *Pkd1* homozygous cell death specifically, with no effect on WT or *Pkd1* heterozygous renal epithelial cells. It has been reported that FoxM1 can regulate apoptosis through the NF-κB signaling pathway (18). To

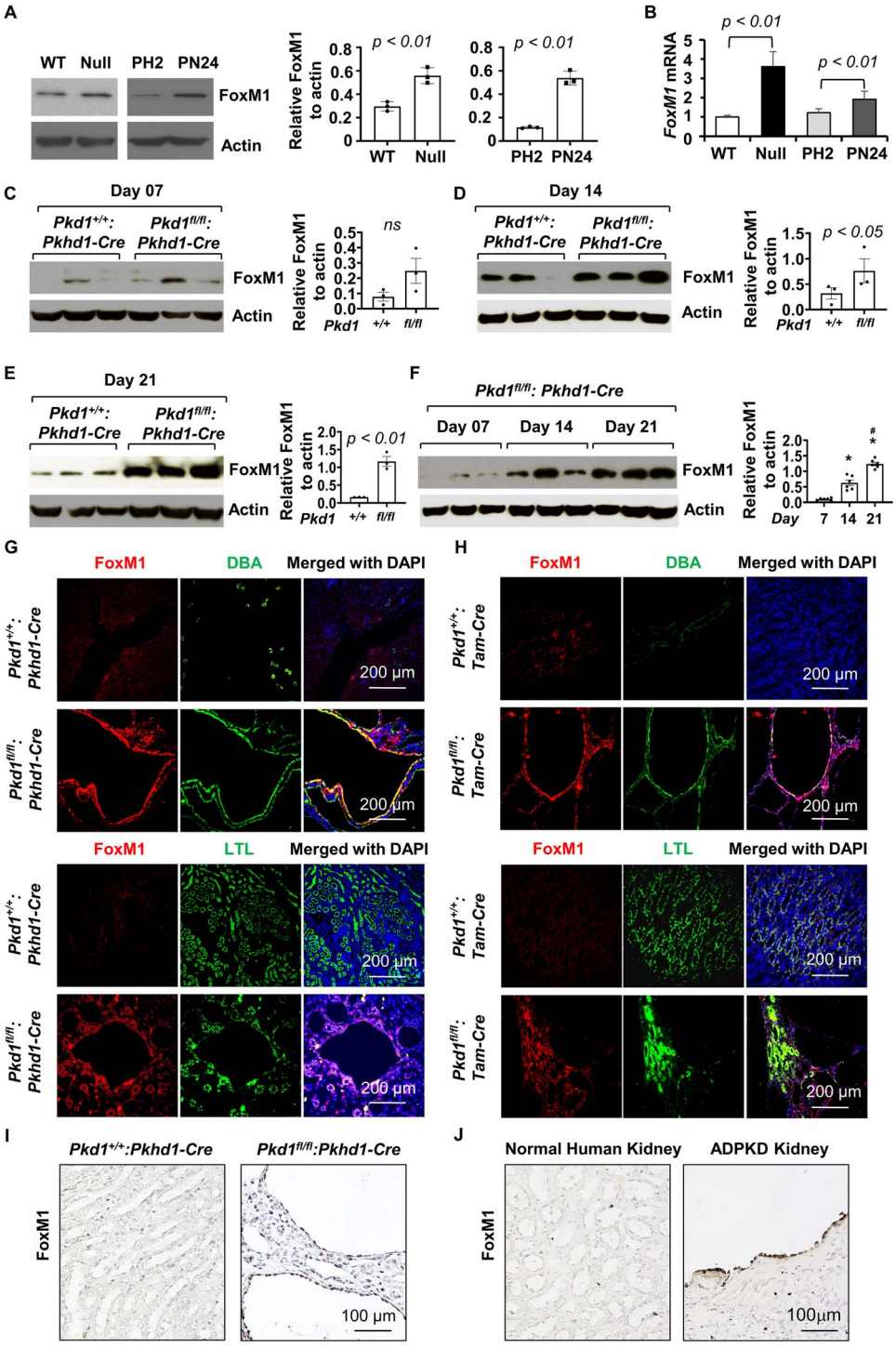

Figure 1. *Pkd1* mutant renal epithelial cells and tissues demonstrated increased expression of FoxM1. (**A**) Western blot analysis of FoxM1 expression from whole cell lysates in *Pkd1* WT, $Pkd1^{null/null}$ MEK cells (Null), *Pkd1*-heterozygous PH2 cells, and *Pkd1*-homozygous PN24 cells. Representative data from three independent experiments are shown. The quantitative and statistical analysis ($n = 3$) of band intensities were showed in the graphs, in that the density of each protein band was normalized to actin (*right panel*). (**B**) qRT-PCR analysis of relative FoxM1 mRNA expression in WT, Null, PH2 and PN24 cells. $n = 3$. (**C**–**E**) Western blot analysis of FoxM1 protein in days 7, 14 and 21 $Pkd1^{+/+}$:*Pkhd1-Cre* (WT) and $Pkd1^{fl/fl}$:*Pkhd1-Cre* (*HOMO*) kidneys ($n = 3$ of each time point). The quantitative and statistical analysis of the band intensities were shown in the graphs, in that the density of each protein band was normalized to actin (*right panel in C–E*). (**F**) Western blot analysis of FoxM1 levels in three kidneys from *Pkd1 HOMO* mice ($n = 3$) at three stages. We repeated this experiment in another three kidneys from *Pkd1 HOMO* mice and we included the quantitative and statistical analysis of the FoxM1 levels in total six *Pkd1 HOMO* kidneys at each time point in *right panel*. ∗ represents the comparison between *HOMO* 7 kidneys with *HOMO* 14 and 21 kidneys, respectively ($P < 0.01$), and # represents the comparison between *HOMO* 14 kidneys with *HOMO* kidneys ($P < 0.05$), as calculated by a one-way ANOVA test. (**G**, **H**) Representative images of immunofluorescence staining indicated that FoxM1 expression was increased in $Pkd1^{fl/fl}$:*Pkhd1-Cre* kidneys (G) and $Pkd1^{fl/fl}$:*Tam-Cre* mice (H) compared to *Pkd1* WT kidneys, co-stained with DBA (*top panel*), LTL (*bottom panel*) and DAPI. Scale bars: 200 μm. Representative data from three independent experiments are shown. (**I** and **J**) IHC analysis of FoxM1, indicating that FoxM1 is upregulated in cyst-lining epithelial cells in kidneys from $Pkd1^{fl/fl}$:*Pkhd1-Cre* mice (I, *right panel*) and ADPKD patients (J, *right panel*) but not that in kidneys from $Pkd1^{+/+}$:*Pkhd1-Cre* mice and normal human kidneys (*left panel*). Representative image from three *PKD1* mutant ADPKD patients was shown in J. Scale bars: 100 μm. Animal data are representative of three independent experiments. *P* values were calculated by one-way ANOVA test in A, B.

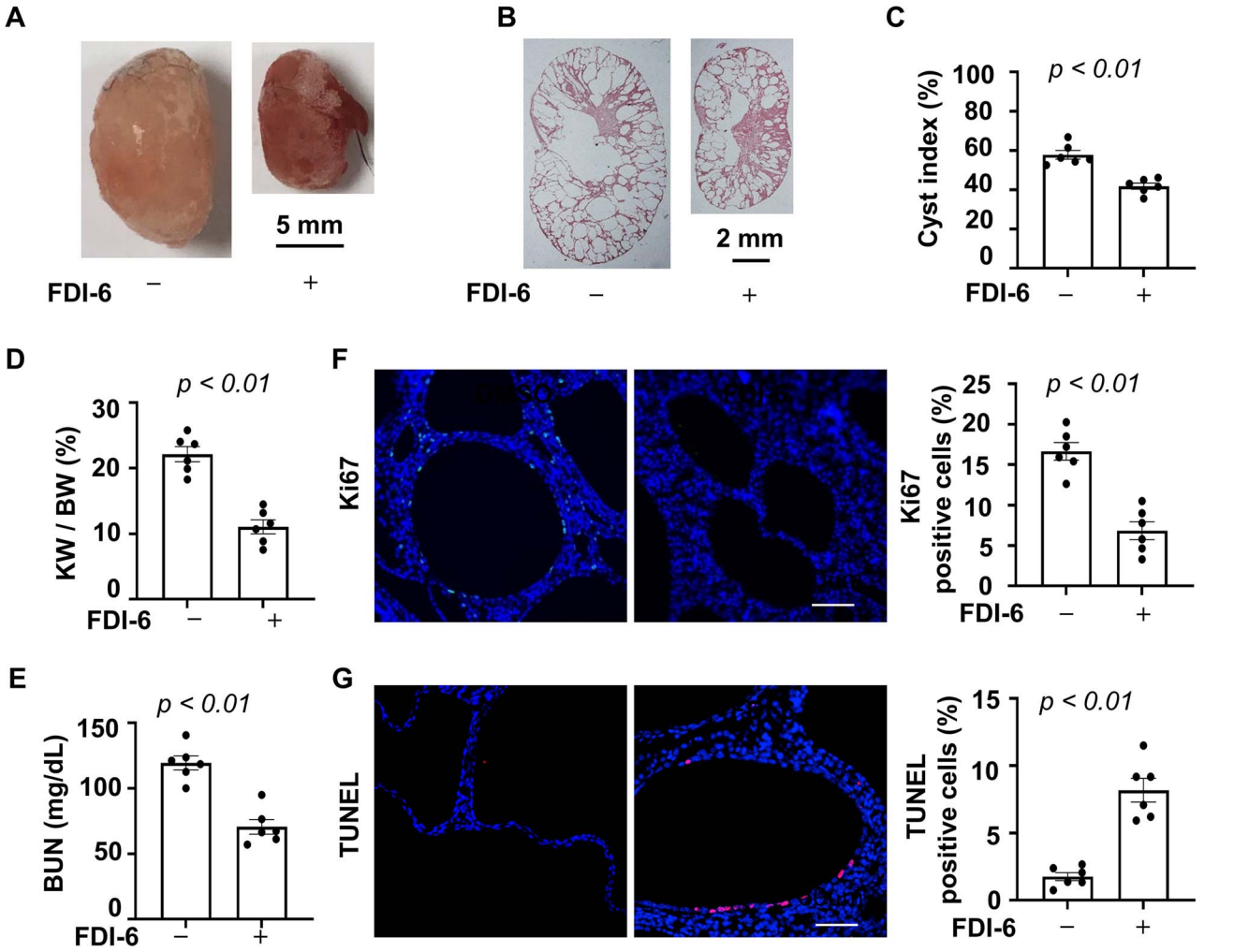

Figure 2. FDI-6 treatment delayed cyst growth in *Pkd1*-knockout mice. (**A**, **B**) Histological examination of kidneys from *Pkd1*$^{nl/nl}$ mice injected daily with FDI-6 or DMSO vehicle control from P7 to P21. (A) Gross pathology of kidneys. Scale bar: 5 mm. (B) Hematoxylin and eosin (H&E) staining, scale bar: 2 mm. Representative image was shown. $n = 6$. (**C**) Percent cystic area relative to total kidney area of kidneys from *Pkd1*$^{nl/nl}$ mice treated with FDI-6 ($n = 6$) or DMSO ($n = 6$). Three male and three female animals were used for all experiments, and comparable experimental results were obtained with each sex. (**D**, **E**) Treatment with FDI-6 compared with DMSO decreased KW/BW ratios (D) and BUN levels (E) in *Pkd1*$^{nl/nl}$ mice. $n = 6$. (**F**) FDI-6 treatment reduced cyst-lining epithelial cell proliferation in kidneys from *Pkd1*$^{nl/nl}$ mice, as detected with Ki67 staining. The percentage of Ki67-positive nuclei in cystic epithelial cells was calculated from an average of 1000 nuclei per mouse kidney section. It was calculated as Ki67 positive cyst-lining epithelial cells/total cyst-lining epithelial cells x 100%, and five images of each animal were counted, $n = 6$ animals were scored. Scale bars: 50 μm. (**G**) FDI-6 treatment induced cyst-lining epithelial cell death in kidneys from *Pkd1*$^{nl/nl}$ mice as detected by TUNEL assay. It was calculated as TUNEL-positive cyst-lining epithelial cells/total cyst-lining epithelial cells x 100%, and five images of each animal were counted, $n = 6$ animals were scored. Scale bars: 50 μm. The *P*-values in B–F were compared FDI-6 treated to DMSO treated mouse kidneys as calculated by one-way ANOVA test.

understand whether targeting FoxM1 with FDI-6 regulates *Pkd1* mutant renal epithelial cell death through NF-κB signaling, we found that inhibition of FoxM1 with FDI-6 significantly induced *Pkd1* homozygous PN24 cell apoptosis as analyzed by TUNEL assay (Fig. 5A). However, inhibition of NF-κB with BAY-11-7085 significantly increased apoptosis induced by FDI-6 treatment in PN24 cells (Fig. 5A, *top panel*). To further determine the dependence of FDI-6 mediated apoptosis on NF-κB signaling, we tried to test the effect of NF-κB activator on FDI-6 mediated apoptosis. However, there is a lack of a specific NF-κB activator. Thus far, the commercially available NF-κB activators, including PMA, betulinic acid and prostratin, are through activating PKC and targeting other mediators to activate NF-κB, and all these compounds have severe side effects on cell survival in addition to activation of NF-κB, which cannot be used in this study (19–21). Our previous study has shown that recombinant TNFα activates NF-κB signaling and results in cell survival (22). Thus, we used recombinant TNFα to activate NF-κB and found that treatment with TNFα alone did not induce cell death in PN24 cells, whereas treatment with TNFα decreased FDI-6 induced apoptosis of PN24 cells compared to those cells treated with FDI-6 alone (Fig. 5A). Treatment with FDI-6 also decreased the expression of p65 and active caspase-3 in *Pkd1* mutant PN24 cells (Fig. 5C). These results suggest that targeting FoxM1 may induce cystic epithelial cell apoptosis via NF-κB signaling.

Treatment with FDI-6 decreases the accumulation of macrophages at interstitial and pericystic regions in *Pkd1* mutant mouse kidneys

It has been reported that the recruitment of macrophages to interstitial and pericystic regions contributes to cyst growth in kidneys in PKD mouse models (5,14,17). We found that treatment with FDI-6 dramatically reduced the recruitment and/or accumulation of macrophages to pericystic sites and interstitial regions in

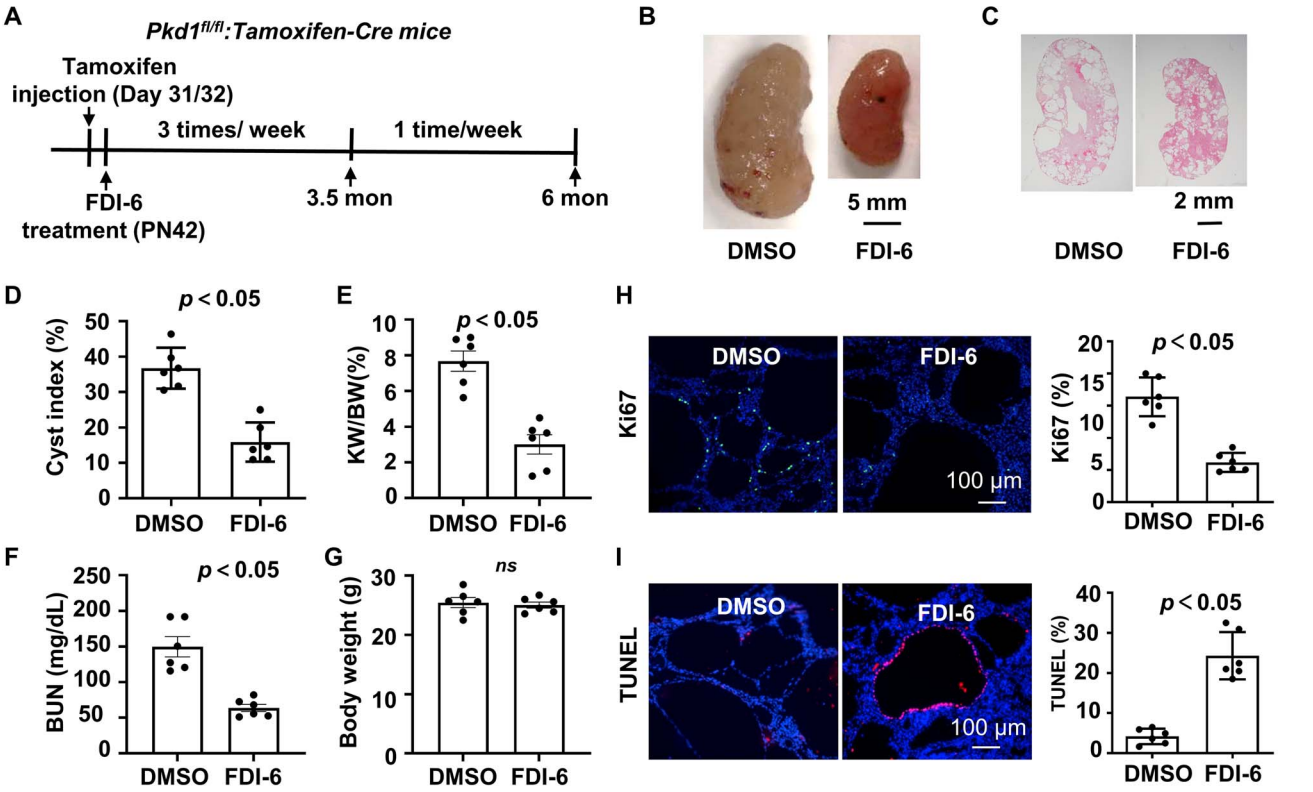

Figure 3. Treatment with FDI-6 delayed cyst growth in *Pkd1*$^{fl/fl}$*:Tam-Cre* mice. (**A**) Schedule of the induction and treatment of *Pkd1* inducible knockout mice. The *Pkd1*$^{fl/fl}$*:Tam-Cre* mice were treated three times per week starting 10 days (PN42) after Pkd1 deletion up to 3.5 months and only one time per week during 3.5 months to 6 months. (**B**, **C**) Histological examination of kidneys from *Pkd1*$^{fl/fl}$*:Tam-Cre* mice injected with FDI-6 ($n = 6$) or DMSO vehicle control ($n = 6$) from P42 to 6 months. Scale bar: 5 mm. (C) H&E staining scale bar: 2 mm. (**D**) Percent cystic area relative to total kidney section area of kidneys from *Pkd1*$^{fl/fl}$*:Tam-Cre* mice treated with FDI-6 ($n = 6$) or DMSO ($n = 6$). (**E**, **F**) Treatment with FDI-6 compared with DMSO decreased KW/BW ratios (E) and BUN levels (F) in *Pkd1*$^{fl/fo}$*:Tam-Cre* mice. (**G**) Treatment with FDI-6 had no effect on the body weights of these mouse models compared to the controls. $n = 6$. (**H**) FDI-6 treatment reduced cyst-lining epithelial cell proliferation in kidneys from *Pkd1*$^{fl/fl}$*:Tam-Cre* mice as detected with Ki67 staining. The percentage of Ki67-positive nuclei in cystic epithelial cells was calculated from an average of 1000 nuclei per mouse kidney section. Scale bars: 100 μm. (*I*) FDI-6 treatment induced cyst-lining epithelial cell death in kidneys from *Pkd1*$^{fl/fl}$*:Tam-Cre* mice as detected by TUNEL assay. Scale bars: 100 μm. There were three male and three female animals used for all experiments, and the comparable experimental results were obtained with each sex. The *P*-value in D–F, H, and I was calculated between FDI-6 and DMSO treated mouse kidneys by one-way ANOVA test.

kidneys from *Pkd1*$^{nl/nl}$ mice and *Pkd1*$^{fl/fl}$*:Tam-Cre* mice, as compared to kidneys from DMSO treated control mice (Fig. 6A and B). These results suggest that there is a role for FoxM1 in regulating the recruitment of macrophages to pericystic sites and interstitial regions in ADPKD kidneys.

Treatment with FDI-6 decreases the expression of MCP-1 in *Pkd1* mutant renal epithelial cells and *Pkd1* $^{fl/fl}$*:Tam-Cre* mouse kidneys

Accumulation of macrophages was associated with increased expression of monocyte chemotactic protein 1 (MCP-1) in the kidneys of Han:SPRD polycystic rats, a nonorthologous model of ADPKD (23). MCP-1 has been reported to be involved in macrophage recruitment and cyst formation (14). We found that the expression of MCP-1 was increased in *Pkd1* homozygous PN24 cells and *Pkd1*$^{fl/fl}$*:Tam-Cre* mouse kidneys compared to *Pkd1* heterozygous PH2 cells and control kidneys (14). Treatment with FDI-6 decreased the expression of MCP-1 in PN24 cells (Fig. 6C) and *Pkd1*$^{fl/fl}$*:Tam-Cre* mouse kidneys (Fig. 6D and E) as examined by qRT-PCR and Western blot analysis and by IHC staining in kidneys from *Pkd1*$^{fl/fl}$*:Tam-Cre* mice compared to untreated controls (Fig. 6F). Our results suggest that FoxM1 is an upstream regulator of MCP-1, and thus that FoxM1 might regulate the recruitment of macrophages to pericystic regions in cystic kidneys via MCP-1.

Discussion

FOXM1 is required for a wide spectrum of essential biological functions, including cell proliferation, cell cycle progression, DNA damage repair, cell renewal, cell differentiation and tissue homeostasis. Its potential as a target for future cancer treatment led to it being designated the 2010 Molecule of the Year (24). However, the functional role and mechanisms of FoxM1 in ADPKD have not been explored. In this study, we have shown that FoxM1 is upregulated in *Pkd1* mutant renal epithelial cells and tissues. Targeting FoxM1 with its specific inhibitor FDI-6 delayed cyst growth in rapidly progressing, early stage and more slowly progressing, milder *Pkd1* mutant mouse models. We further showed that FoxM1 regulates cyst growth through (1) the activation of several PKD-associated signaling pathways, including Akt, ERK, Rb and Stat3, promoting the expression of Cdk6, CyclinD1 and Plk1 to increase cystic renal epithelial cell proliferation; (2) the induction of the expression and activation of NF-κB to repress cystic renal epithelial cell apoptosis; and (3) the recruitment of macrophages at interstitial and pericystic regions in *Pkd1* conditional knockout mouse kidneys, a process that is likely to be regulated by FoxM1-mediated the upregulation of MCP-1 (Fig. 7). These results support the idea that FoxM1 plays a critical role in promoting of ADPKD progression and thus may be a novel therapeutic target for ADPKD treatment.

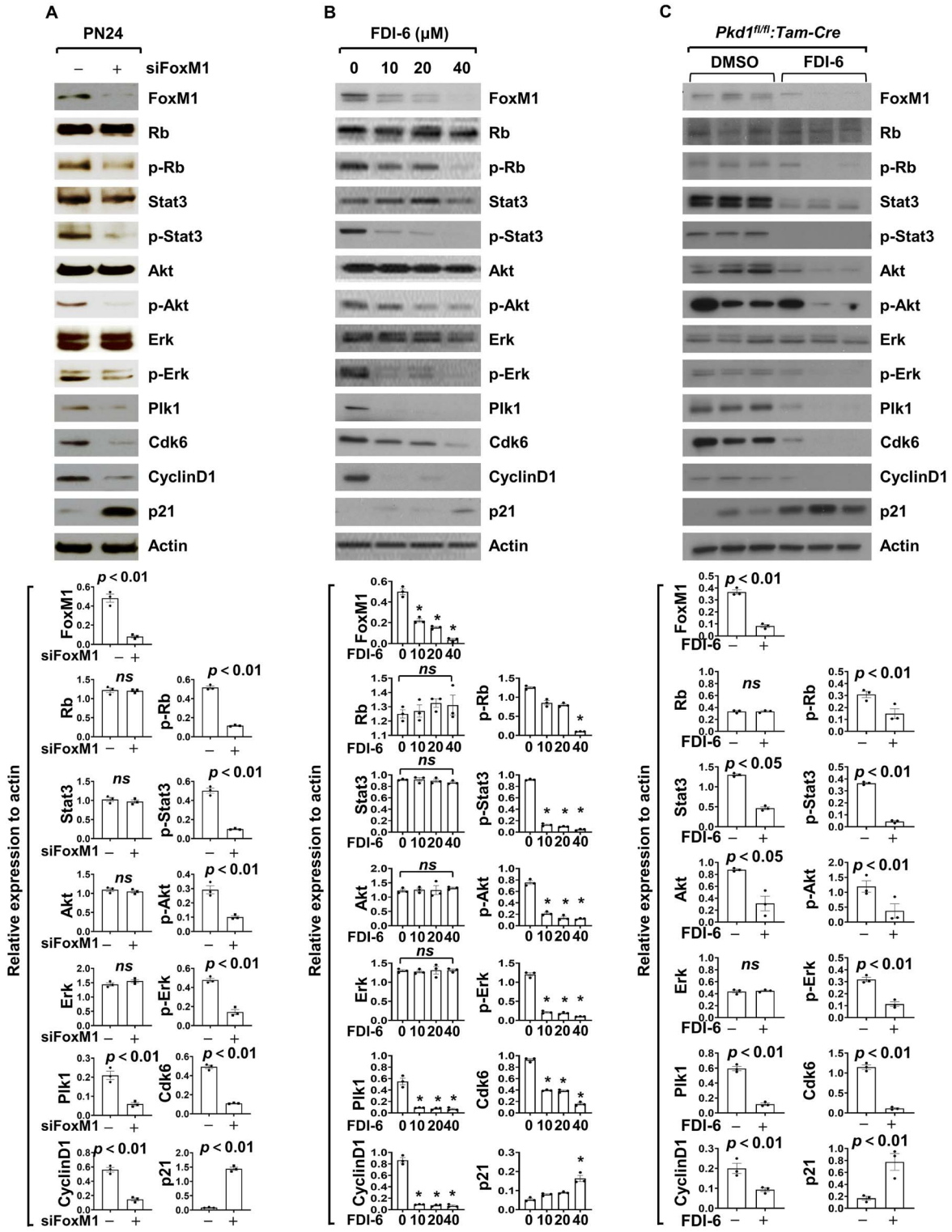

Figure 4. Suppression of FDI-6 normalized PKD associated signaling pathways in *Pkd1* mutant renal epithelial cells and tissues. (**A**) Western blot analysis of the expression and phosphorylation of Rb, Akt, Stat3, ERK, Plk1, Cdk6, Cyclin D1 and p21 in PN24 cells treated with or without siRNA of FoxM1 for 48 h. Data are representative of three independent experiments. Statistical analysis of the expression ($n = 3$) of these proteins was shown in the graphs (*bottom panel*). The *P*-value was compared siRNA FoxM1 treated to siRNA control treated PN24 cells as calculated by one-way ANOVA test. (**B**) Western blot analysis of the expression and phosphorylation of ERK, Akt, Stat3, Rb, Plk1, Cdk6, Cyclin D1 and p21 in PN24 cells treated with or without FDI-6 for 24 h. Data are representative of three independent experiments ($n = 3$), and the statistical analysis of the expression of these proteins is shown in the graphs (*bottom panel*). $*$ represents the comparison of these proteins in PN24 cells without FDI-6 treatment (0 μM) to those cells treated with 10, 20 and 40 μM FDI-6 as calculated by a one-way ANOVA test ($P < 0.01$). (**C**) Western blot analysis of the expression and phosphorylation of PKD associated proteins in *Pkd1*$^{fl/fl}$*:Tam-Cre* mouse kidneys treated with FDI-6 compared to those in DMSO control treated mice. Representative data from three independent experiments are shown ($n = 3$), and the statistical analysis of the expression of these proteins is shown in the graphs (*bottom panel*). *P*-values were calculated by one-way ANOVA test.

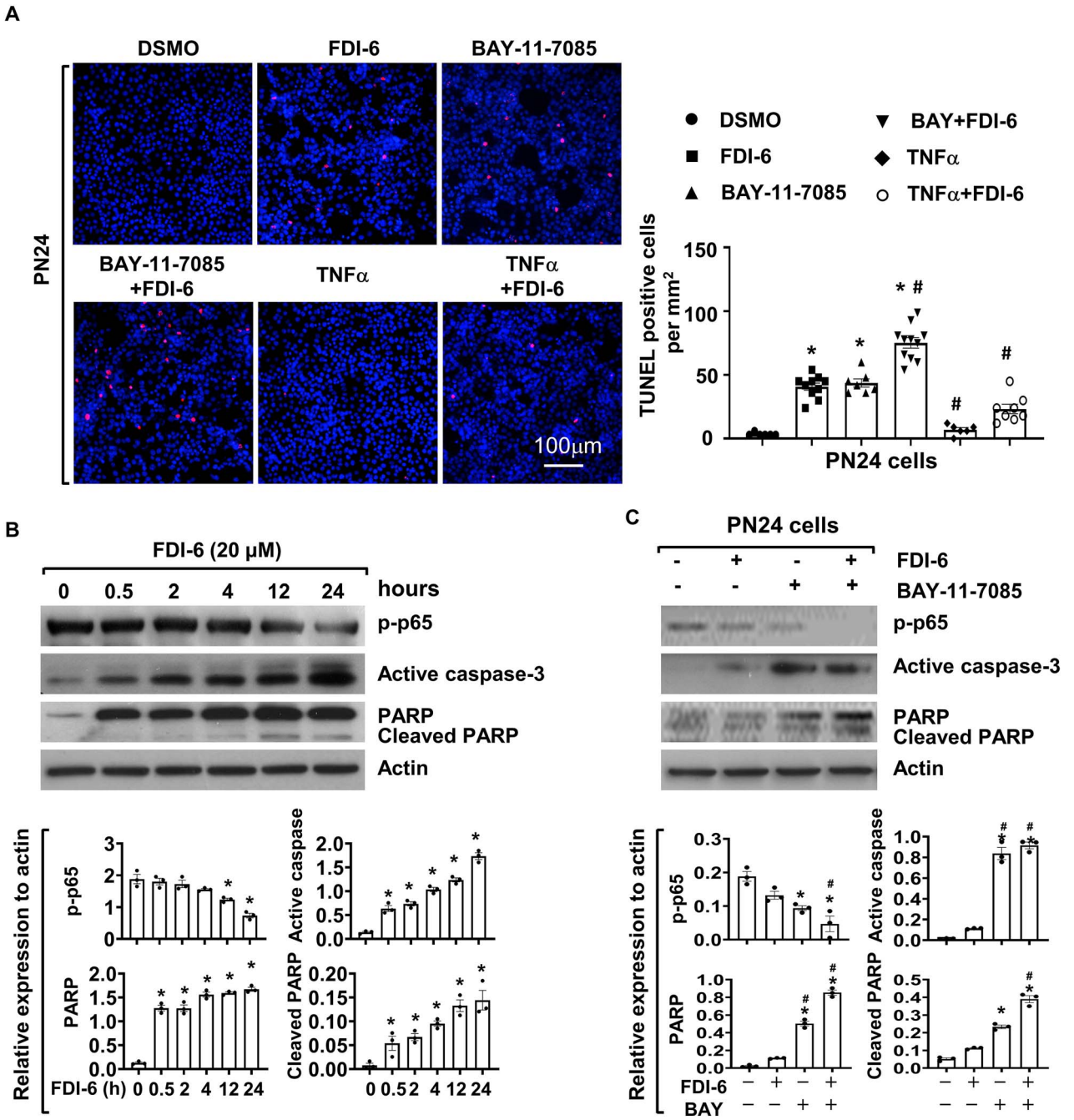

Figure 5. Inhibition of FoxM1 induces cystic epithelial cell apoptosis via NF-κB. (**A**) NF-κB was involved in FoxM1 mediated cell death in renal epithelial cells. Treatment with FoxM1 inhibitor FDI-6 alone or NF-κB inhibitor BAY-11-7085 alone induced renal epithelial cell death in *Pkd1* homozygous PN24 cells, treatment with both FDI-6 and BAY-11-7085 induced more cell death in PN24 cells compared to those in FDI-6 and BAY-11-7085 alone treated cells, whereas treatment with TNFα blocked FDI-6 induced cell death as detected by TUNEL assay. Scale bar: 100 μm. Data are representative of three independent experiments. Statistical analysis of apoptotic cells treated with FDI-6 alone or co-treatment with NF-κB inhibitors/activators is shown in the graphs (*right panel*). $*$ indicates $P < 0.05$ as compared to cells with no treatment, # indicates $P < 0.05$ as compared to the FDI-6 treated cells. *P* values were calculated by one-way ANOVA test. (**B**) Western blot analysis of the expression of phosphorylated p65 (p-p65) and active caspase-3, as well as the cleaved poly (ADP-ribose) polymerase (PARP), a substrate of caspase-3 in *Pkd1*-homozygous PN24 cells treated with FDI-6 (20 μM) at the indicated time points. The expression of active caspase-3, as well as the cleaved PARP, was gradually increased in PN24 cells treated with FDI-6 up to 24 h, while the expression of phosphorylated p65 was gradually decreased in the same ones, compared with untreated cells (0 h). The quantitative and statistical analysis of the levels of these proteins ($n = 3$) is shown in the bottom panels. $*$ represents the comparison of these proteins in PN24 cells without FDI-6 treatment (0 h) to those cells treated with FDI-6 for 0.5, 2, 4, 12 and 24 h, as calculated by a one-way ANOVA test ($P < 0.01$). (**C**) Western blot analysis of the expression of phosphorylated p65 and active caspase-3 in PN24 cells treated with FDI-6 (20 μM) combined with or without BAY-11-7085 (20 μM) for 24 h. Representative data from three independent experiments are shown. $*$ represents the comparison of these proteins in PN24 cells without FDI-6 or BAY-11-7085 treatment to those cells treated with FDI-6, BAY-11-7085 or both FDI-6 and BAY-11-7085 ($P < 0.01$), and # represents the comparison between FDI-6 treated cells with cells treated with BAY-11-7085 or both FDI-6 and BAY-11-7085 ($P < 0.05$), as calculated by a one-way ANOVA test.

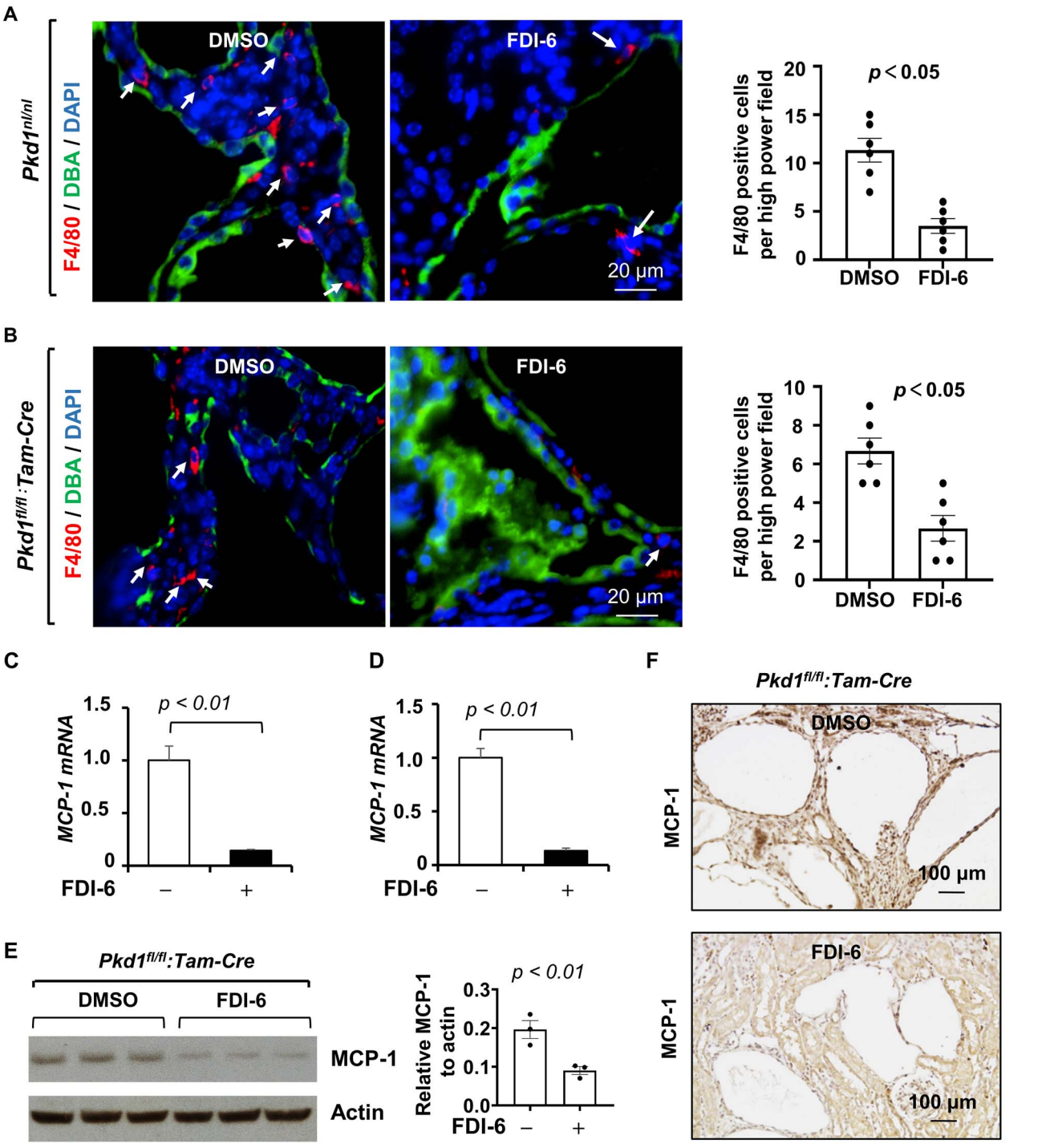

Figure 6. Treatment with FDI-6 decreases the expression of MCP-1 and macrophage accumulation in pericystic and interstitial regions of *Pkd1* conditional knockout mouse kidneys. (**A** and **B**) The accumulation/recruitment of macrophages to pericystic sites and interstitium in kidneys from $Pkd1^{nl/nl}$ mice ($n=6$) (A) and $Pkd1^{fl/fl}$:*Tam-Cre* mice ($n=6$) (B) was dramatically reduced compared to that from age matched $Pkd1^{nl/nl}$ mice and $Pkd1^{fl/fl}$:*Tam-Cre* mice treated with DMSO. Scale bar: 20 μm. (**C**–**E**) The expression levels of MCP-1 mRNA (C and D) and protein (E) were decreased in *Pkd1* homozygous PN24 cells (C) and $Pkd1^{fl/fl}$:*Tam-Cre* mouse kidneys (D) with treatment of FDI-6 compared to DMSO vehicle as examined by qRT-PCR and western blot analysis (E). The statistical analysis of the expression of MCP-1 in three kidneys from $Pkd1^{fl/fl}$:*Tam-Cre* mice ($n=3$) was shown in the graphs (*right panel*). (**F**) MCP-1 expression was decreased in $Pkd1^{fl/fl}$:*Tam-Cre* mouse kidney tissues as examined by immunohistochemical staining with anti-MCP-1 antibody in $Pkd1^{fl/fl}$:*Tam-Cre* mice. Data are representative of three independent experiments. *P*-values were calculated by one-way ANOVA test in A–D.

Increased expression of FOXM1 is observed in a variety of human cancers, including ovarian cancer, breast cancer, prostate cancer, hepatoma, angiosarcoma, colorectal cancer, melanoma, lung cancer and gastric cancer, and dysregulation of FOXM1 is associated with almost all hallmarks of tumor cells (13). In this study, we report for the first time that FOXM1 is upregulated in ADPKD kidneys. To understand the mechanism for the dysregulation of FOXM1 in cystic kidneys, we examined the core promoter of the FOXM1 gene and found that it contains several regulatory elements, including E-boxes, and other cis-acting elements that

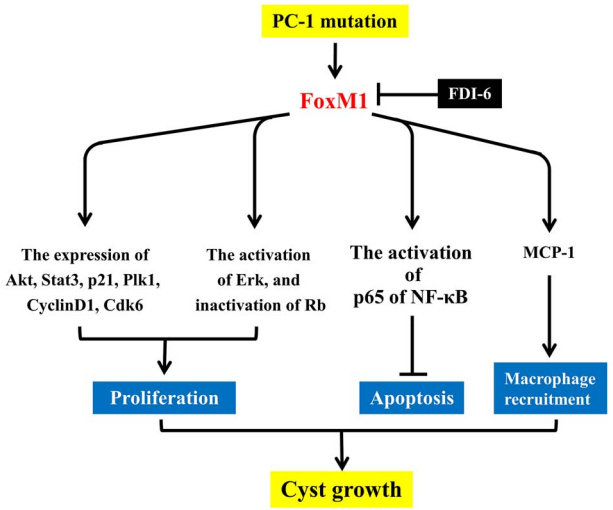

Figure 7. Working model for FoxM1 in the regulation of cyst growth in ADPKD. A schematic diagram depicting FoxM1-mediated pathways in *Pkd1* mutant renal epithelial cells and kidneys. *Pkd1* mutation results in the upregulation of FoxM1 and upregulated FoxM1 (i) increases *Pkd1* mutant renal epithelial cell proliferation through the regulation of the expression and the phosphorylation and/or activation of Akt, ERK, Rb and Stat3 signaling as well as the expression of Cdk6, cyclin D1, p21 and Plk1; (ii) decreases *Pkd1* mutant renal epithelial cell apoptosis through NF-κB signaling and (iii) is responsible for the recruitment of macrophages to pericystic and interstitial regions in *Pkd1* mutant mouse kidneys, a process likely to be enhanced by FoxM1-mediated upregulation of MCP-1. Targeting FoxM1 with its specific inhibitor, FDI-6, delays cyst growth in *Pkd1* mutant mouse kidneys.

can function as response elements for other transcription factors, such as cAMP responsive element-binding protein (CREB), CCCTC-binding factor (CTCF), glioma-associated oncogene homolog 1 (Gli1) (25–27), signal transducer and activator of transcription 3 (STAT3) and E2F. These factors interact directly with their binding sites to positively regulate FOXM1 expression (28–30). Importantly, all these factors have been associated with the regulation of cyst progression in ADPKD animal models (16,31,32), supporting the idea that a direct interaction between these factors and their binding sites may contribute to the upregulation of FOXM1 in *Pkd1* mutant renal epithelial cells. In addition, FOXM1 can be regulated post-transcriptionally by microRNAs (miRNAs), the endogenous, highly conserved, non-coding RNAs of approximately 21–24 nucleotides that can guide mRNA degradation or repress translation by binding to complementary sequences in the 3′ untranslated regions (3'UTRs) of targeted mRNAs (13). Several miRNAs have been identified that promote cyst growth in ADPKD and the targeting of miRNAs can delay cyst progression (33). A comprehensive understanding of the regulation of FOXM1 expression by known and novel transacting factors at the FOXM1 promoter should provide novel insights into FoxM1 signaling in ADPKD that will facilitate the development of therapeutic strategies for the inhibition of FOXM1 and its regulators.

As a classic proliferation-associated transcription factor, FOXM1 directly or indirectly activates the expression of a network of proliferation-associated target genes at the transcriptional level to regulate the cell cycle, including G1/S phase transition, mitotic spindle assembly, chromosome segregation and G2/M transition (24,34,35). Once activated, FOXM1 promotes G1/S phase transition or S phase progression by activating the transcription of genes regulating the G1/S checkpoint (36). For example, FoxM1 can regulate the transcription of Skp2 and Cks1, which are required for targeting p21(Cip1) and p27(Kip1) for degradation during G1/S phase transition (36). FoxM1 regulates G2/M transition or M phase entry through the elevation of the transcription of genes regulating the G2/M checkpoint, including PLK1, CDC25B, CCNB1, NEK2 and BIRC5 [37–39]. In addition, FOXM1 promotes faithful mitotic progression by activating genes involved in mitotic spindle assembly and chromosome segregation, such as Aurora B kinase (AURKB), KIF20A, centromere protein A (CENPA), CENPB and CENPF (36). Our results show that FOXM1 regulates the expression of PLK1, CyclinD1, CDK6 and p21, and the activation of signaling intermediates, including but not limited to Akt, Erk, Rb and Stat3, in the regulation of cystic epithelial cell proliferation and disease progression. Targeting FOXM1 with its inhibitor FDI-6 normalized the expression of those genes and perhaps other signaling intermediates to delay cyst growth in *Pkd1* mutant kidneys.

In the past decades, an increasing number of studies have demonstrated that apoptosis plays an essential role in the regulation of cystogenesis in ADPKD. However, whether apoptosis is increased or decreased in ADPKD kidneys, and whether induction of apoptotic cell death promotes, or delays cyst growth has remained controversial (22). In addition to promoting cell proliferation, overexpression of FoxM1 inhibits apoptosis in hypopharyngeal squamous cell carcinoma, resulting in a poor clinical prognosis (37). Previous studies demonstrated that FoxM1 can regulate apoptosis through the NF-κB signaling pathway (18), and that targeting NF-κB and FOXM1 with panepoxydone inhibits proliferation but induces apoptosis in breast cancer (38). In addition, FOXM1 depletion sensitizes both normal keratinocytes and squamous cell carcinoma cells to ROS-induced apoptosis, suggesting that squamous cell carcinoma cells may use FOXM1 to control oxidative stress to escape premature senescence and apoptosis (39). FoxM1 knockdown was also seen to sensitize human cancer cells to apoptotic cell death induced by proteasome inhibitors, such as, MG132, bortezomib and thiostrepton, while it did not affect the levels of autophagy following treatment with these drugs (40). Our results support the notion that FoxM1 can regulate cystic epithelial cell apoptosis through the NF-κB signaling pathway and the idea that targeting FoxM1-induced apoptosis may contribute to delay cyst growth in ADPKD kidneys.

The roles of the inflammation response in the pathogenesis of ADPKD have become a focus of research in the past decade (14,41–43). Accumulating evidence supports the idea that interstitial macrophages promote cyst growth in human ADPKD and rodent cystic models (42,44). It has been shown that depletion of macrophages can delay cyst growth and improve renal function in *Pkd1* mutant mouse kidneys. Our group further found that macrophage migration inhibitory factor (MIF) regulated the recruitment of macrophages to pericystic regions as well as regulating other signaling pathways to promote cyst growth in *Pkd1* mutant mice (14). It has been reported that FoxM1 is required for macrophage migration during lung inflammation and tumor formation (45). Knockdown of FOXM1 attenuates the inflammatory response in human osteoarthritis chondrocytes (46). Moreover, FOXM1 silencing has been shown to inhibit the generation of inflammatory cytokines induced by lipopolysaccharides (LPS), including IL-1β, IL-6 and TNFα (47), and pharmacologic inhibition of FoxM1 was shown to reduce liver inflammation in models of liver injury. Liver inflammation was associated with increased levels of hepatic and serum chemokine (C-C motif) ligand 2 (CCL2), which is also referred to as MCP-1, and *in vitro* transcriptional analysis confirmed that CCL2 is a direct target of FoxM1 in murine hepatocytes (48). Our results showed that targeting FoxM1 decreases the expression of MCP-1 and the recruitment of macrophages in *Pkd1* mutant

kidneys, suggesting that FoxM1-mediated expression of cytokines, such as MCP-1, IL-1 and 6 and TNFα, may be an alternative mechanism for the recruitment of macrophages in ADPKD kidneys.

Pharmacological inhibition of FOXM1 expression and/or its interactions with target sites (by blocking the DBD, nuclear localization or protein–protein interaction) should be an effective way to inhibit FOXM1-mediated biological effects. Over the last decade, significant progress has been made in the inhibition of FOXM1 in cancer therapy (13). Several recent studies have found that small molecule inhibitors work well to inhibit FOXM1 (49). Among those small FOXM1 inhibitors, FDI-6 has been characterized in depth and has been shown to bind directly to FOXM1 protein in a 1:1 stoichiometry to reversibly block its DNA binding activity and to displace FOXM1 from chromatin and genomic targets, resulting in a concomitant transcriptional down-regulation of FOXM1-activated genes as well as the pathways known to be controlled by FoxM1 transactivation (49), including transcriptional down-regulation of FOXM1 itself. It is worth noting that there is a positive autoregulation loop for FOXM1 (50), which was demonstrated by two transcriptional inhibitors of FOXM1, siomycin A and thiostrepton, that downregulated both the transcriptional activity and expression levels of FOXM1 (50). Our current study has also shown that FDI-6 can downregulate both the transcriptional activity and expression levels of FOXM1. The promise that FDI-6 shows with its anti-tumor activities (51) and in delaying cyst growth suggests that it has the potential to be developed as a novel treatment for ADPKD. Although much work has been done, there is much more to accomplish to validate FDI-6 in clinical trials, as a single agent or in combination for ADPKD treatment.

Materials and Methods

Cell culture and reagents

Pkd1 WT and *Pkd1* null MEK cells, which were derived from collecting ducts and sorted using the collecting duct marker *dolichos biflorus* agglutinin (DBA) from kidneys of WT and *Pkd1*-null mice, were generated from Jing Zhou's laboratory at Harvard Medical School (Boston, MA, USA), which were maintained as previously described in our recent publications (14,16,17). *Pkd1* heterozygous PH2 cells and homozygous PN24 cells were provided by Stefan Somlo through the George M. O'Brien Kidney Center at Yale University (New Haven, CT, USA) and were cultured as described (14). FDI-6 was purchased from AXON MEDCHEM (Catalogue ID:2384) and dissolved in DMSO (Sigma-Aldrich) as a stock solution of 20 mM. PN24 cells were treated with FDI-6 for 24 h, and then were harvested and analyzed by Western blot. BAY-11-7085 was purchased from Cayman Chemical and dissolved in DMSO (Sigma-Aldrich) as a stock solution of 20 mM. All stock solutions were stored at −20°C.

Antibodies used for Western blot analysis included (a) anti-FoxM1 (sc-502), anti-STAT3 (sc-482), anti-p65 (sc372 and sc-8008), anti-p21 (sc-53 870), anti-CyclinD1 (sc-8396) and anti-Plk1(sc-17 783) purchased from Santa Cruz Biotechnology Inc.; (b) anti-ERK (no. 4696), anti-Rb (no.9309) and anti-AKT (no. 9272) purchased from Cell Signaling Technology; and (c) the antibodies for phosphorylated STAT3-Y705 (no. 9131), p65-S536 (no. 3031), ERK-T202/Y204 (no. 9101), AKT-S473 (no. 9271) and Rb-S780 (no. 9307), also purchased from Cell Signaling Technology.

Western blot analysis

Cell pellets were collected and resuspended in lysis buffer (20 mM Tris-HCl, pH 7.4, 150 mM NaCl, 10% glycerol, 1% Triton X-100, 1 mM Na_3VO_4, 25 mM β-glycerol phosphate, 0.1 mM PMSF, Roche complete protease inhibitor set, and Sigma-Aldrich phosphatase inhibitor set). The resuspended cell pellet was vortexed for 20 s and then incubated on ice for 30 min and centrifuged at 20 000 g for 30 min. The supernatants were collected for Western blot analysis.

Histology and IHC

Kidneys were fixed with 4% paraformaldehyde (pH 7.4). Paraffin-embedded sections (5 μm) were subjected to H&E staining and IHC. For FoxM1 staining, a polyclonal goat anti-FoxM1 antibody (Santa Cruz Biotechnology Inc.; 1:100 dilution), biotinylated secondary antibody (Santa Cruz Biotechnology Inc.; 1:100 dilution) and DAB substrate system were used. Kidney sections were counterstained by hematoxylin. Images were analyzed with a Nikon TI2-E microscope.

IF staining

For Ki67 staining, a rabbit anti-Ki67 antibody (ab15580; Abcam) and Alexa Fluor 488 anti-rabbit IgG secondary antibody were used. Macrophages were detected by IF staining with a pan-macrophage marker, F4/80. After antigen retrieval, tissue sections were incubated with a rat anti-mouse F4/80 antibody (14-4801-82; eBioscience Inc.; 1:100 dilution) overnight, and then were incubated with Fluro-555 anti-rat IgG secondary antibody and mounted in Prolong Gold Antifade reagent with DAPI (Invitrogen). Images were analyzed using a Nikon TI2-E microscope.

Quantitative reverse-transcription PCR

Total RNA was extracted using the RNeasy Plus Mini Kit (QIAGEN). Total RNA (1 μg) was used for RT reactions in a 20-μl reaction to synthesize cDNA using an iScript cDNA Synthesis Kit (Bio-Rad). RNA expression profiles were analyzed by real-time PCR using iTaq SYBR Green Supermix with ROX (Bio-Rad) in an iCycler iQ Real-Time PCR Detection System. The complete reactions were subjected to the following program of thermal cycling: 40 cycles of 10 s at 95°C and 20 s at 60°C. A melting curve was run after the PCR cycles, followed by a cooling step. Each sample was run in triplicate in each experiment, and each experiment was repeated three times. Expression levels of target genes were normalized to the expression level of actin. Genes were amplified using the following primers: FoxM1-F, 5′-ATCGCTACTTGACATTGGACC-3′; FoxM1-R, 5′-CAGTGGGATTTCAGTTTTGATGG-3′; Mcp-1-F, 5′- GTCCCTGTCATGCTTCTGG-3′; Mcp-1-R, 5′- GCTCTCCAGCCTACTCATTG-3′; actin-F, 5′-AAGAGCTATGAGCTGCCTGA-3′; actin-R, 5′-TACGGATGTCAACGTCACAC-3′.

TUNEL assay

TUNEL assays for homozygous PN24 cells with FDI-6 or DMSO or BAY-11-7085 or combined with FDI-6 as well as TNFα or combined with FDI-6, and kidneys treated with FDI-6 or DMSO were performed according to the manufacturer's protocols (In Situ Death Detection Kit; Roche Diagnostics). ProLong Gold Antifade reagent with DAPI (Invitrogen) was used. IF images were obtained with a Nikon TI2-E microscope.

Mouse strains and treatments

Hypomorphic $Pkd1^{nl/nl}$ mice, generated by cross-breeding $Pkd1^{nl/+}$ females with $Pkd1^{nl/+}$ males, were used to test the effects of FDI-6 on cyst progression at postnatal day 28 (P28). $Pkd1^{nl/nl}$ pups were injected i.p. with FDI-6 (5 mg/kg, dissolved in DMSO, with a final DMSO concentration of 10% [v/v] in PBS) or DMSO (control) daily

from postnatal day 7 (P7) to postnatal day 27 (P27), and kidneys and serum were collected at P28, 24 h after last dose as described in our publication (52).

Pkd1$^{fl/fl}$ mice (B6; 129S4-*Pkd1*^{tm2Ggg}/J; stock 010671; Jackson Laboratory) possess loxP sites on either side of exons 2–4 of *Pkd1* (53). *Pkd1*$^{fl/fl}$:*Pkhd1-Cre* mice were generated by cross-breeding *Pkd1*$^{fl/+}$:*Pkhd1-Cre* female mice with *Pkd1*$^{fl/+}$:*Pkhd1-Cre* male mice.

Pkd1$^{fl/fl}$:*tamoxifen-Cre* mice were generated by cross-breeding *Pkd1*$^{fl/fl}$ female mice with *Esr1*$^{+}$ *-Cre* male mice (Esr1-Cre, stock #: 017911, Jackson Laboratory), in which the Cre is driven by the *Esr1*$^{+}$ promoter (54). These mice were treated with tamoxifen (125 mg/kg body weight, formulated in corn oil) by daily intraperitoneal (IP) injection on two sequential postnatal days (P31 and P32) to induce *Pkd1* deletion in the test group. Ten days (P42) after *Pkd1* deletion, *Pkd1*$^{fl/fl}$:*tamoxifen-Cre* mice were treated with FDI-6 (10 mg/kg body weight) with (1) a three-times-per-week schedule from day 42 to 3.5 months, and (2) an one-time-per-week schedule from 3.5 to 6 months. We collected blood samples 24 h after the last dose and harvested kidneys from 6-month-old FDI-6- and vehicle-treated (DMSO-treated) mice for histopathological and biochemical analysis.

We treated hypomorphic *Pkd1*$^{nl/nl}$ mice and *Pkd1*$^{fl/fl}$:*tamoxifen-Cre* mice with FDI-6 by using i.p. injection for two reasons: (1) comparing with oral administration, administration of FDI-6 to animals with i.p. injection was more efficient, and (2) the amount of FDI-6 administered to animals was more controllable. In addition, three male and three female animals were used for all experiments, and comparable experimental results were obtained with each sex.

Measurement of cyst area

The cyst volume was quantified in whole kidney after H&E staining using Image-Pro Plus v5 software (Media Cybernetics). The cyst area was calculated as (cyst area/total area) × 100 Three sections from both kidneys were analyzed for each mouse.

Quantitative BUN determination

Serum samples were first diluted 5-fold in distilled water prior to assay. Next, 5 μl water (blank), 5 μl standard (50 mg/dl) and 5 μl sample were transferred in triplicate into wells of a clear-bottom 96-well plate. Approximately 200 μl of working reagent was added and tapped lightly to mix, and the samples were incubated 20 min at room temperature. Optical density was read at 520 nm.

Statistics

All data are presented as mean ± SEM. All statistical analyses were performed using SPSS Statistics 22 software. *P* values were calculated by teo-tailed unpaired Student's *t*-test and one-way ANOVA; and a *P*-value less than 0.05 was considered significant.

Study approval

All animal protocols were approved by and conducted in accordance with Laboratory Animal Resources of Mayo Clinic and Institutional Animal Care and Use Committee regulations.

Funding

X.L. acknowledges support from National Institutes of Health (grant R01 DK129241, R01 DK126662), and from the PKD Foundation. J.P.C. acknowledges support from National Institutes of Health (U54 DK126126).

Competing Interests

The authors have declared that no completing interest exists.

Authors' Contributions

W.Y. and G.W. performed most of the experiments and data analysis, L.X.L. X.G. and J.X.Z performed some of the experiments and data analysis. J.P.C. assisted in data analysis and manuscript preparation. X.L. supervised the whole project, data analysis and manuscript writing.

References

1. Torres, V.E. and Harris, P.C. (2011) Polycystic kidney disease in 2011: connecting the dots toward a polycystic kidney disease therapy. *Nat. Rev. Nephrol.*, **8**, 66–68.
2. Peters, D.J. and Sandkuijl, L.A. (1992) Genetic heterogeneity of polycystic kidney disease in Europe. *Contrib. Nephrol.*, **97**, 128–139.
3. Torres, V.E. and Harris, P.C. (2014) Strategies targeting cAMP signaling in the treatment of polycystic kidney disease. *J. Am. Soc. Nephrol.*, **25**, 18–32.
4. Sun, Y., Zhou, H. and Yang, B.X. (2011) Drug discovery for polycystic kidney disease. *Acta Pharmacol. Sin.*, **32**, 805–816.
5. Li, X. (2011) Epigenetics and autosomal dominant polycystic kidney disease. *Biochim. Biophys. Acta*, **1812**, 1213–1218.
6. Zhang, X., Li, L.X., Ding, H., Torres, V.E., Yu, C. and Li, X. (2021) Ferroptosis promotes cyst growth in autosomal dominant polycystic kidney disease mouse models. *J. Am. Soc. Nephrol.*, **32**, 2759–2776.
7. Chen, L., Wei, Q., Bi, S. and Xie, S. (2020) Maternal embryonic leucine zipper kinase promotes tumor growth and metastasis via stimulating FOXM1 signaling in esophageal squamous cell carcinoma. *Front. Oncol.*, **10**, 10.
8. He, H., Chen, J., Zhao, J., Zhang, P., Qiao, Y., Wan, H., Wang, J., Mei, M., Bao, S. and Li, Q. (2021) PRMT7 targets of Foxm1 controls alveolar myofibroblast proliferation and differentiation during alveologenesis. *Cell Death Dis.*, **12**, 841.
9. Gartel, A.L. (2017) FOXM1 in cancer: interactions and vulnerabilities. *Cancer Res.*, **77**, 3135–3139.
10. Littler, D.R., Alvarez-Fernandez, M., Stein, A., Hibbert, R.G., Heidebrecht, T., Aloy, P., Medema, R.H. and Perrakis, A. (2010) Structure of the FoxM1 DNA-recognition domain bound to a promoter sequence. *Nucleic Acids Res.*, **38**, 4527–4538.
11. O'Regan, R.M. and Nahta, R. (2018) Targeting forkhead box M1 transcription factor in breast cancer. *Biochem. Pharmacol.*, **154**, 407–413.
12. Laissue, P. (2019) The forkhead-box family of transcription factors: key molecular players in colorectal cancer pathogenesis. *Mol. Cancer*, **18**, 5.
13. Liao, G.B., Li, X.Z., Zeng, S., Liu, C., Yang, S.M., Yang, L., Hu, C.J. and Bai, J.Y. (2018) Regulation of the master regulator FOXM1 in cancer. *Cell Commun. Signal*, **16**, 57.
14. Chen, L., Zhou, X., Fan, L.X., Yao, Y., Swenson-Fields, K.I., Gadjeva, M., Wallace, D.P., Peters, D.J., Yu, A., Grantham, J.J. and Li, X. (2015) Macrophage migration inhibitory factor promotes cyst growth in polycystic kidney disease. *J. Clin. Invest.*, **125**, 2399–2412.
15. Perez, D.J., Amirhossein Tabatabaei Dakhili, S., Bergman, C., Dufour, J., Wuest, M., Juengling, F.D., Wuest, F. and Velazquez-Martinez, C.A. (2021) FOXM1 inhibitors as potential diagnostic agents: first generation of a PET probe targeting FOXM1 to detect

triple-negative breast cancer in vitro and in vivo. *Chem Med Chem*, **16**, 3720–3729.
16. Li, L.X., Fan, L.X., Zhou, J.X., Grantham, J.J., Calvet, J.P., Sage, J. and Li, X. (2017) Lysine methyltransferase SMYD2 promotes cyst growth in autosomal dominant polycystic kidney disease. *J. Clin. Invest.*, **127**, 2751–2764.
17. Zhou, X., Fan, L.X., Sweeney, W.E., Jr., Denu, J.M., Avner, E.D. and Li, X. (2013) Sirtuin 1 inhibition delays cyst formation in autosomal-dominant polycystic kidney disease. *J. Clin. Invest.*, **123**, 3084–3098.
18. Zhou, M., Shi, J., Lan, S. and Gong, X. (2021) FOXM1 regulates the proliferation, apoptosis and inflammatory response of keratinocytes through the NF-kappaB signaling pathway. *Hum. Exp. Toxicol.*, **40**, 1130–1140.
19. Kasperczyk, H., La Ferla-Bruhl, K., Westhoff, M.A., Behrend, L., Zwacka, R.M., Debatin, K.M. and Fulda, S. (2005) Betulinic acid as new activator of NF-kappaB: molecular mechanisms and implications for cancer therapy. *Oncogene*, **24**, 6945–6956.
20. Holden, N.S., Squires, P.E., Kaur, M., Bland, R., Jones, C.E. and Newton, R. (2008) Phorbol ester-stimulated NF-kappaB-dependent transcription: roles for isoforms of novel protein kinase C. *Cell. Signal.*, **20**, 1338–1348.
21. Jiang, G. and Dandekar, S. (2015) Targeting NF-kappaB signaling with protein kinase C agonists as an emerging strategy for combating HIV latency. *AIDS Res. Hum. Retrovir.*, **31**, 4–12.
22. Fan, L.X., Zhou, X., Sweeney, W.E., Jr., Wallace, D.P., Avner, E.D., Grantham, J.J. and Li, X. (2013) Smac-mimetic-induced epithelial cell death reduces the growth of renal cysts. *J. Am. Soc. Nephrol.*, **24**, 2010–2022.
23. Cowley, B.D., Jr., Ricardo, S.D., Nagao, S. and Diamond, J.R. (2001) Increased renal expression of monocyte chemoattractant protein-1 and osteopontin in ADPKD in rats. *Kidney Int.*, **60**, 2087–2096.
24. Li, Y., Wu, F., Tan, Q., Guo, M., Ma, P., Wang, X., Zhang, S., Xu, J., Luo, P. and Jin, Y. (2019) The multifaceted roles of FOXM1 in pulmonary disease. *Cell Commun. Signal*, **17**, 35.
25. Torres, V.E., Chapman, A.B., Devuyst, O., Gansevoort, R.T., Grantham, J.J., Higashihara, E., Perrone, R.D., Krasa, H.B., Ouyang, J., Czerwiec, F.S. and TEMPO 3:4 Trial Investigators (2012) Tolvaptan in patients with autosomal dominant polycystic kidney disease. *N. Engl. J. Med.*, **367**, 2407–2418.
26. Torres, V.E., Higashihara, E., Devuyst, O., Chapman, A.B., Gansevoort, R.T., Grantham, J.J., Perrone, R.D., Ouyang, J., Blais, J.D., Czerwiec, F.S. and TEMPO 3:4 Trial Investigators (2016) Effect of tolvaptan in autosomal dominant polycystic kidney disease by CKD stage: results from the TEMPO 3:4 trial. *Clin. J. Am. Soc. Nephrol.*, **11**, 803–811.
27. Torres, V.E., Chapman, A.B., Devuyst, O., Gansevoort, R.T., Perrone, R.D., Koch, G., Ouyang, J., McQuade, R.D., Blais, J.D., Czerwiec, F.S., Sergeyeva, O. and REPRISE Trial Investigators (2017) Tolvaptan in later-stage autosomal dominant polycystic kidney disease. *N. Engl. J. Med.*, **377**, 1930–1942.
28. Millour, J., de Olano, N., Horimoto, Y., Monteiro, L.J., Langer, J.K., Aligue, R., Hajji, N. and Lam, E.W. (2011) ATM and p53 regulate FOXM1 expression via E2F in breast cancer epirubicin treatment and resistance. *Mol. Cancer Ther.*, **10**, 1046–1058.
29. Mencalha, A.L., Binato, R., Ferreira, G.M., Du Rocher, B. and Abdelhay, E. (2012) Forkhead box M1 (FoxM1) gene is a new STAT3 transcriptional factor target and is essential for proliferation, survival and DNA repair of K562 cell line. *PLoS One*, **7**, e48160.
30. Xia, L., Huang, W., Tian, D., Zhu, H., Zhang, Y., Hu, H., Fan, D., Nie, Y. and Wu, K. (2012) Upregulated FoxM1 expression induced by hepatitis B virus X protein promotes tumor metastasis and indicates poor prognosis in hepatitis B virus-related hepatocellular carcinoma. *J. Hepatol.*, **57**, 600–612.
31. Moisan, S., Levon, S., Cornec-Le Gall, E., Le Meur, Y., Audrezet, M.P., Dostie, J. and Ferec, C. (2018) Novel long-range regulatory mechanisms controlling PKD2 gene expression. *BMC Genomics*, **19**, 515.
32. Ma, M., Legue, E., Tian, X., Somlo, S. and Liem, K.F., Jr. (2019) Cell-autonomous hedgehog signaling is not required for cyst formation in autosomal dominant polycystic kidney disease. *J. Am. Soc. Nephrol.*, **30**, 2103–2111.
33. Woo, Y.M., Kim, D.Y., Koo, N.J., Kim, Y.M., Lee, S., Ko, J.Y., Shin, Y., Kim, B.H., Mun, H., Choi, S. *et al.* (2017) Profiling of miRNAs and target genes related to cystogenesis in ADPKD mouse models. *Sci. Rep.*, **7**, 14151.
34. Saldivar, J.C., Hamperl, S., Bocek, M.J., Chung, M., Bass, T.E., Cisneros-Soberanis, F., Samejima, K., Xie, L., Paulson, J.R., Earnshaw, W.C. *et al.* (2018) An intrinsic S/G2 checkpoint enforced by ATR. *Science*, **361**, 806–810.
35. Vaz, S., Ferreira, F.J., Macedo, J.C., Leor, G., Ben-David, U., Bessa, J. and Logarinho, E. (2021) FOXM1 repression increases mitotic death upon antimitotic chemotherapy through BMF upregulation. *Cell Death Dis.*, **12**, 542.
36. Filliol, A. and Schwabe, R.F. (2020) FoxM1 induces CCl2 secretion from hepatocytes triggering hepatic inflammation, injury, fibrosis, and liver cancer. *Cell. Mol. Gastroenterol. Hepatol.*, **9**, 555–556.
37. Chen, Y., Liu, Y., Ni, H., Ding, C., Zhang, X. and Zhang, Z. (2017) FoxM1 overexpression promotes cell proliferation and migration and inhibits apoptosis in hypopharyngeal squamous cell carcinoma resulting in poor clinical prognosis. *Int. J. Oncol.*, **51**, 1045–1054.
38. Hamurcu, Z., Sener, E.F., Taheri, S., Nalbantoglu, U., Kokcu, N.D., Tahtasakal, R., Cinar, V., Guler, A., Ozkul, Y., Donmez-Altuntas, H. *et al.* (2021) MicroRNA profiling identifies Forkhead box transcription factor M1 (FOXM1) regulated miR-186 and miR-200b alterations in triple negative breast cancer. *Cell. Signal.*, **83**, 109979.
39. Choi, H.S., Kim, Y.K., Hwang, K.G. and Yun, P.Y. (2020) Increased FOXM1 expression by cisplatin inhibits paclitaxel-related apoptosis in cisplatin-resistant human oral squamous cell carcinoma (OSCC) cell lines. *Int. J. Mol. Sci.*, **21**.
40. Gopalakrishnan, S. and Ismail, A. (2021) Aromatic monophenols from cinnamon bark act as proteasome inhibitors by upregulating ER stress, suppressing FoxM1 expression, and inducing apoptosis in prostate cancer cells. *Phytother. Res.*, **35**, 5781–5794.
41. Li, X., Magenheimer, B.S., Xia, S., Johnson, T., Wallace, D.P., Calvet, J.P. and Li, R. (2008) A tumor necrosis factor-alpha-mediated pathway promoting autosomal dominant polycystic kidney disease. *Nat. Med.*, **14**, 863–868.
42. Swenson-Fields, K.I., Vivian, C.J., Salah, S.M., Peda, J.D., Davis, B.M., van Rooijen, N., Wallace, D.P. and Fields, T.A. (2013) Macrophages promote polycystic kidney disease progression. *Kidney Int.*, **83**, 855–864.
43. Sadasivam, M., Noel, S., Lee, S.A., Gong, J., Allaf, M.E., Pierorazio, P., Rabb, H. and Hamad, A.R.A. (2019) Activation and proliferation of PD-1(+) kidney double-negative T cells is dependent on non-classical MHC proteins and IL-2. *J. Am. Soc. Nephrol.*, **30**, 277–292.
44. Karihaloo, A., Koraishy, F., Huen, S.C., Lee, Y., Merrick, D., Caplan, M.J., Somlo, S. and Cantley, L.G. (2011) Macrophages promote cyst growth in polycystic kidney disease. *J. Am. Soc. Nephrol.*, **22**, 1809–1814.
45. Yuan, Q., Wen, M., Xu, C., Chen, A., Qiu, Y.B., Cao, J.G., Zhang, J.S. and Song, Z.W. (2019) 8-bromo-7-methoxychrysin targets

NF-kappaB and FoxM1 to inhibit lung cancer stem cells induced by pro-inflammatory factors. *J. Cancer*, **10**, 5244–5255.
46. Zeng, R.M., Lu, X.H., Lin, J., Hu, J., Rong, Z.J., Xu, W.C., Liu, Z.W. and Zeng, W.T. (2019) Knockdown of FOXM1 attenuates inflammatory response in human osteoarthritis chondrocytes. *Int. Immunopharmacol.*, **68**, 74–80.
47. Zeng, R., Lu, X., Lin, J., Ron, Z., Fang, J., Liu, Z. and Zeng, W. (2021) FOXM1 activates JAK1/STAT3 pathway in human osteoarthritis cartilage cell inflammatory reaction. *Exp. Biol. Med.*, **246**, 644–653.
48. Kurahashi, T., Yoshida, Y., Ogura, S., Egawa, M., Furuta, K., Hikita, H., Kodama, T., Sakamori, R., Kiso, S., Kamada, Y. *et al.* (2020) Forkhead Box M1 transcription factor drives liver inflammation linking to hepatocarcinogenesis in mice. *Cell. Mol. Gastroenterol. Hepatol.*, **9**, 425–446.
49. Gormally, M.V., Dexheimer, T.S., Marsico, G., Sanders, D.A., Lowe, C., Matak-Vinkovic, D., Michael, S., Jadhav, A., Rai, G., Maloney, D.J. *et al.* (2014) Suppression of the FOXM1 transcriptional programme via novel small molecule inhibition. *Nat. Commun.*, **5**, 5165.
50. Halasi, M. and Gartel, A.L. (2009) A novel mode of FoxM1 regulation: positive auto-regulatory loop. *Cell Cycle*, **8**, 1966–1967.
51. Ulhaka, K., Kanokwiroon, K., Khongkow, M., Bissanum, R., Khunpitak, T. and Khongkow, P. (2021) The anticancer effects of FDI-6, a FOXM1 inhibitor, on triple negative breast cancer. *Int. J. Mol. Sci.*, **22**.
52. Li, L.X., Zhang, L., Agborbesong, E., Zhang, X., Zhou, J.X. and Li, X. (2022) Cross talk between lysine methyltransferase Smyd2 and TGF-beta-Smad3 signaling promotes renal fibrosis in autosomal dominant polycystic kidney disease. *Am. J. Physiol. Renal Physiol.*, **323**, F227–F242.
53. Shibazaki, S., Yu, Z., Nishio, S., Tian, X., Thomson, R.B., Mitobe, M., Louvi, A., Velazquez, H., Ishibe, S., Cantley, L.G. *et al.* (2008) Cyst formation and activation of the extracellular regulated kinase pathway after kidney specific inactivation of Pkd1. *Hum. Mol. Genet.*, **17**, 1505–1516.
54. Lee, H., Kim, D.W., Remedios, R., Anthony, T.E., Chang, A., Madisen, L., Zeng, H. and Anderson, D.J. (2014) Scalable control of mounting and attack by Esr1+ neurons in the ventromedial hypothalamus. *Nature*, **509**, 627–632.